Control of Spinning Symmetric Airframes*

Curtis P. Mracek† Max Stafford‡and Mike Unger §
Raytheon Systems Company
Tucson, AZ 85734

Several missiles and projectiles have periods during their flight where the body is spinning and must be controlled. It has been stated that a roll stabilized autopilot may be more appropriate during this phase of the flight.[5] This paper first examines the full nonlinear equations of motion in both the roll stabilized frame and the body axis system assuming a rigid axially symmetric body. Two and three loop autopilots are developed using an optimal control approach for a non rolling airframe. These autopilots are examined to determine how well they are able to follow inertial commands. An extremely simplified example is presented so that the basic characteristics of the closed loop system can be examined. The results are presented and conclusions drawn. Effects of different acceleration levels, including the axial moment of inertia and very high roll rates are examined.

I. Introduction

Several missiles and projectiles have periods during their flight where the body is spinning and must be controlled. This paper develops the full nonlinear equations of motion in both the body and what is called the roll stabilized coordinate frames. The roll stabilized frame is a frame where the Euler roll rate is always zero. Four autopilot topologies were examined for control of a rolling airframe. These were the classical three loop implemented in the body axis system, the classical three loop implemented in a roll stabilized system and a two loop autopilot implemented in both the body and roll stabilized frames. It is shown the two loop implementations are identical. There is no advantage of using the roll stabilized coordinate frame for the two loop design. The three loop autopilots produce significantly different results. An extremely simplified numerical example is presented so that the basic characteristics of the closed loop system can be examined. Results are presented and discussed. Finally conclusions are reached.

II. Coordinate Frames and Notation

There are three coordinate frames used in the derivation of the equations of motion. There is the inertial frame designated with and "I", the roll stabilized frame labeled "ϕ" and the body frame designated "B". The inertial frame is the frame in which Newtons Equations of Motion can be applied. The roll stabilized frame is defined such that the Euler angular rate is zero for all time ($\dot{\phi} = 0$). The body frame is attached to the spinning body. The unit vector triplets $(\hat{\imath}_X, \hat{\jmath}_X, \hat{k}_X)$ will be used for each coordinate system. The rotation sequence from the inertial to the roll stabilized frame is first through a rotation about the inertial z axis through the heading angle Ψ. Using an intermediate coordinate system "1". The second rotation is about the intermediate y axis through the angle Θ. The direction cosine matrix is

$$\begin{bmatrix} \hat{\imath}_\phi \\ \hat{\jmath}_\phi \\ \hat{k}_\phi \end{bmatrix} = \begin{bmatrix} \cos(\Theta) & 0 & -\sin(\Theta) \\ 0 & 1 & 0 \\ \sin(\Theta) & 0 & \cos(\Theta) \end{bmatrix} \begin{bmatrix} \cos(\Psi) & \sin(\Psi) & 0 \\ -\sin(\Psi) & \cos(\Psi) & 0 \\ 0 & 0 & 1 \end{bmatrix} \begin{bmatrix} \hat{\imath}_1 \\ \hat{\jmath}_1 \\ \hat{k}_1 \end{bmatrix}$$

*This paper is approved for public release; distribution is unlimited.
†Engineering Fellow, Raytheon, Senior Member AIAA
‡Raytheon, Member AIAA
§Raytheon

Report Documentation Page

Form Approved
OMB No. 0704-0188

1. REPORT DATE	2. REPORT TYPE	3. DATES COVERED
14 NOV 2006	**N/A**	**-**

4. TITLE AND SUBTITLE	5a. CONTRACT NUMBER
Control of Spinning Symmetric Airframes	5b. GRANT NUMBER
	5c. PROGRAM ELEMENT NUMBER
6. AUTHOR(S)	5d. PROJECT NUMBER
	5e. TASK NUMBER
	5f. WORK UNIT NUMBER
7. PERFORMING ORGANIZATION NAME(S) AND ADDRESS(ES) **Raytheon Systems Company Tucson, AZ 85734**	8. PERFORMING ORGANIZATION REPORT NUMBER
9. SPONSORING/MONITORING AGENCY NAME(S) AND ADDRESS(ES)	10. SPONSOR/MONITOR'S ACRONYM(S)
	11. SPONSOR/MONITOR'S REPORT NUMBER(S)

12. DISTRIBUTION/AVAILABILITY STATEMENT
Approved for public release, distribution unlimited

13. SUPPLEMENTARY NOTES
See also ADM202095. Proceedings of the 2006 AIAA Missile Sciences Conference Held in Monterey, California on 14-16 November 2006

14. ABSTRACT

15. SUBJECT TERMS

16. SECURITY CLASSIFICATION OF:			17. LIMITATION OF ABSTRACT	18. NUMBER OF PAGES	19a. NAME OF RESPONSIBLE PERSON
a. REPORT **unclassified**	b. ABSTRACT **unclassified**	c. THIS PAGE **unclassified**	**SAR**	**23**	

The angular velocity between the systems (read as the angular velocity of frame "ϕ" relative to "I") is

$$\vec{\omega}_{\phi/I} = \dot{\Psi}\hat{k}_I + \dot{\Theta}\hat{\jmath}_\phi = p\hat{\imath}_\phi + q\hat{\jmath}_\phi + r\hat{k}_\phi$$

The body axis system is arrived through one more rotation about the roll stabilized x axis. That is

$$\begin{bmatrix} \hat{\imath}_B \\ \hat{\jmath}_B \\ \hat{k}_B \end{bmatrix} = C_{B/\phi} \begin{bmatrix} \hat{\imath}_\phi \\ \hat{\jmath}_\phi \\ \hat{k}_\phi \end{bmatrix}$$

where

$$C_{B/\phi} = \begin{bmatrix} 1 & 0 & 0 \\ 0 & \cos(\Phi) & \sin(\Phi) \\ 0 & -\sin(\Phi) & \cos(\Phi) \end{bmatrix}$$

and the angular velocity of the body frame relative to the roll stabilized frame is

$$\vec{\omega}_{B/\phi} = \dot{\Phi}\hat{\imath}_\phi$$

There is absolutely nothing special about the above definitions. The exact same rotation sequence and equations can be found in Roskam, Blakelock and Etkin. The only difference is the roll stabilized frame was defined as an intermediate frame. The angular velocity of the body frame relative to the inertial frame is

$$\vec{\omega}_{B/I} = \vec{\omega}_{B/\phi} + \vec{\omega}_{\phi/I} = \dot{\Psi}\hat{k}_I + \dot{\Theta}\hat{\jmath}_\phi + \dot{\Phi}\hat{\imath}_B = P\hat{\imath}_B + Q\hat{\jmath}_B + R\hat{k}_B$$

III. Linear Momentum and the Force Equation

The linear momentum of a rolling rigid airframe is

$$\vec{P} = m\,{}^I\vec{V}_{C/O}$$

where the velocity is defined as the time rate of change of the position of the center of mass "C" relative to an inertially fixed point "O" as seen by an inertial observer. The notion will be

$${}^I\vec{V}_{C/O} = \frac{{}^I\mathrm{d}R_{C/O}}{\mathrm{d}t}$$

Newtons Law states that the mass times the acceleration is equal to the sum of the applied external forces. That is

$$\sum \vec{F}_{Ext} = m\frac{{}^I\mathrm{d}\,{}^I\vec{V}_{C/O}}{\mathrm{d}t}$$

The derivative can be expanded using the transport theorem, or

$$\frac{{}^I\mathrm{d}\,{}^I\vec{V}_{C/O}}{\mathrm{d}t} = \frac{{}^B\mathrm{d}\,{}^I\vec{V}_{C/O}}{\mathrm{d}t} + \vec{\omega}_{B/I} \times \vec{V}_{C/O}$$

IV. Angular Momentum and the Moment Equation

The angular momentum about the airframe center of mass of a rotating rigid airframe is

$$\vec{H} = \bar{\bar{I}}_C \cdot \vec{\omega}_{B/I}$$

For an axially symmetric body, the moment of inertia tensor reduces to

$$\bar{\bar{I}}_C = I_{xx}\hat{\imath}_B\hat{\imath}_B + I\hat{\jmath}_B\hat{\jmath}_B + I\hat{k}_B\hat{k}_B$$

This notation may look a little strange, it is simply a tensor notation, the results are the same as for the standard matrix approach only a matrix cross product does not need to be defined. For a rigid body Newtons law reduces to the change in angular momentum is equal to the sum of the external moments, or

$$\sum \vec{M}_{Ext} = \frac{{}^I\mathrm{d}\vec{H}}{\mathrm{d}t}$$

again using the transport theorem

$$\frac{{}^{I}\mathrm{d}\vec{H}}{\mathrm{d}t} = \frac{{}^{B}\mathrm{d}\vec{H}}{\mathrm{d}t} + \vec{\omega}_{B/I} \times \vec{H}$$

V. Body Axis System Equations of Motion

The equations of motion in the body axis system are derived using the body axis variables, the linear velocity is

$${}^{I}\vec{V}_{C/O} = U\hat{\imath}_B + V\hat{\jmath}_B + W\hat{k}_B$$

and the angular velocity is

$$\vec{\omega}_{B/I} = P\hat{\imath}_B + Q\hat{\jmath}_B + R\hat{k}_B$$

The force equation is

$$\frac{\sum \vec{F}_{Ext}}{m} = \dot{U}\hat{\imath}_B + \dot{V}\hat{\jmath}_B + \dot{W}\hat{k}_B + \left(P\hat{\imath}_B + Q\hat{\jmath}_B + R\hat{k}_B\right) \times \left(U\hat{\imath}_B + V\hat{\jmath}_B + W\hat{k}_B\right)$$

or in component form

$$\dot{U} + QW - RV = \frac{F_x}{m}$$
$$\dot{V} + RU - PW = \frac{F_y}{m}$$
$$\dot{W} + PV - QU = \frac{F_z}{m}$$

where the force components are in the body axis system.

The moment equation is

$$\sum \vec{M}_{Ext} = \frac{{}^{I}\mathrm{d}\vec{H}}{\mathrm{d}t}$$

$$\begin{aligned}\sum \vec{M}_{Ext} &= \frac{{}^{I}\mathrm{d}\vec{H}}{\mathrm{d}t} \\ &= \left(I_{xx}\dot{P} + IQR - IQR\right)\hat{\imath}_B + \left(I\dot{Q} + I_{xx}PR - IPR\right)\hat{\jmath}_B \\ &\quad + \left(I\dot{R} + IPQ - I_{xx}PQ\right)\hat{k}_B\end{aligned}$$

or in component form

$$I_{xx}\dot{P} = M_x$$
$$I\dot{Q} + I_{xx}PR - IPR = M_y$$
$$I\dot{R} + IPQ - I_{xx}PQ = M_z$$

where the moment components are in the body axis system.

VI. Roll Stabilized Equations of Motion

The equations of motion in the roll stabilized axis system are derived using the roll stabilized axis variables. The linear velocity is

$${}^{I}\vec{V}_{C/O} = u\hat{\imath}_\phi + v\hat{\jmath}_\phi + w\hat{k}_\phi$$

and the angular velocity is

$$\vec{\omega}_{\phi/I} = p\hat{\imath}_\phi + q\hat{\jmath}_\phi + r\hat{k}_\phi$$

The force equation is

$$\frac{\sum \vec{F}_{Ext}}{m} = \dot{u}\hat{\imath}_\phi + \dot{v}\hat{\jmath}_\phi + \dot{w}\hat{k}_\phi + \left(p\hat{\imath}_\phi + q\hat{\jmath}_\phi + r\hat{k}_\phi\right) \times \left(u\hat{\imath}_\phi + v\hat{\jmath}_\phi + w\hat{k}_\phi\right)$$

or in component form

$$\dot{u} + qw - rv = \frac{f_x}{m}$$
$$\dot{v} + ru - pw = \frac{f_y}{m}$$
$$\dot{w} + pv - qu = \frac{f_z}{m}$$

where the force components are in the roll stabilized system. Clearly the force equation have not been simplified using the local level frame, though it should be noted the roll rate in the roll stabilized system is zero at zero pitch attitude and is significantly smaller for rolling airframes compared to the roll rate of the body axis system. One inconvenience is that the forces are usually written in the body axis system but for a symmetric body this difficulty should be able to be overcome.

The moment equations are

$$\begin{aligned}\sum \vec{M}_{Ext} &= \frac{{}^{I}\mathrm{d}\vec{H}}{\mathrm{d}t} \\ &= \frac{{}^{\phi}\mathrm{d}\vec{H}}{\mathrm{d}t} + \vec{\omega}_{\phi/I} \times \vec{H} \\ &= \frac{{}^{\phi}\mathrm{d}\bar{\bar{I}}_C \cdot \vec{\omega}_{B/I}}{\mathrm{d}t} + \vec{\omega}_{\phi/I} \times \left(\bar{\bar{I}}_C \cdot \vec{\omega}_{B/I}\right)\end{aligned}$$

we must now pause and look at the time rate of change of the inertia tensor as seen by someone in the roll stabilized frame. Fortunately the body is axially symmetric thus using the coordinate transformation of a tensor we find the moment of inertia tensor is

$$\bar{\bar{I}}_C = I_{xx}\hat{\imath}_{\phi L}\hat{\imath}_\phi + I\hat{\jmath}_\phi\hat{\jmath}_\phi + I\hat{k}_\phi\hat{k}_\phi$$

so that it is also invariant seen by the roll stabilized frame, thus

$$\begin{aligned}\sum \vec{M}_{Ext} &= \bar{\bar{I}}_C \cdot \frac{{}^{\phi}\mathrm{d}\vec{\omega}_{B/I}}{\mathrm{d}t} + \vec{\omega}_{\phi/I} \times \left(\bar{\bar{I}}_C \cdot \vec{\omega}_{B/I}\right) \\ &= \bar{\bar{I}}_C \cdot \left(\frac{{}^{B}\mathrm{d}\vec{\omega}_{B/I}}{\mathrm{d}t} + \vec{\omega}_{B/\phi} \times \vec{\omega}_{B/I}\right) + \vec{\omega}_{\phi/I} \times \left(\bar{\bar{I}}_C \cdot \vec{\omega}_{B/I}\right)\end{aligned}$$

now we must either put the local level angular velocity or the body angular velocity vector in a different frame so that the cross products can be taken. Choosing the later

$$\begin{aligned}\vec{\omega}_{B/I} &= P\hat{\imath}_B + Q\hat{\jmath}_B + R\hat{k}_B \\ &= P\hat{\imath}_\phi + \left[Q\cos(\Phi) - R\sin(\Phi)\right]\hat{\jmath}_\phi + \left[Q\sin(\Phi) + R\cos(\Phi)\right]\hat{k}_\phi\end{aligned}$$

therefore

$$\begin{aligned}\sum \vec{M}_{Ext} &= \left(I_{xx}\hat{\imath}_\phi\hat{\imath}_\phi + I\hat{\jmath}_\phi\hat{\jmath}_\phi + I\hat{k}_\phi\hat{k}_\phi\right) \cdot \left(\dot{P}\hat{\imath}_B + \dot{Q}\hat{\jmath}_B + \dot{R}\hat{k}_B\right) \\ &\quad + \left(I_{xx}\hat{\imath}_\phi\hat{\imath}_\phi + I\hat{\jmath}_\phi\hat{\jmath}_\phi + I\hat{k}_\phi\hat{k}_\phi\right) \cdot \left[\dot{\Phi}\hat{\imath}_\phi \times \vec{\omega}_{B/I}\right] \\ &\quad + \left(p\hat{\imath}_\phi + q\hat{\jmath}_\phi + r\hat{k}_\phi\right) \times \left[\left(I_{xx}\hat{\imath}_\phi\hat{\imath}_\phi + I\hat{\jmath}_\phi\hat{\jmath}_\phi + I\hat{k}_\phi\hat{k}_\phi\right) \cdot \vec{\omega}_{B/I}\right]\end{aligned}$$

Substituting using the following identities

$$q = \left[Q\cos(\Phi) - R\sin(\Phi)\right]$$
$$r = \left[Q\sin(\Phi) + R\cos(\Phi)\right]$$

$$\dot{q} = \dot{Q}\cos(\Phi) - \dot{R}\sin(\Phi) - \dot{\Phi}Q\sin(\Phi) - \dot{\Phi}R\cos(\Phi)$$

and

$$\dot{r} = \dot{Q}\sin(\Phi) + \dot{R}\cos(\Phi) + \dot{\Phi}Q\cos(\Phi) - \dot{\Phi}R\sin(\Phi)$$

yields the component equations

$$I_{xx}\dot{p} = m_x$$
$$I\dot{q} + I_{xx}Pr - Ipr = m_y$$
$$I\dot{r} + Ipq - I_{xx}Pq = m_z$$

where the moments are written in the roll stabilized frame.

Notice most of the cross coupling is gone but not all the roll rate of the roll stabilized frame (small but usually nonzero) still produces a cross coupled term and the gyroscopic effects still couple the pitch and yaw channels. The fact that the roll rate of the roll stabilized frame (p) is significantly smaller then the roll rate of the body axis system (P) is the reason to hope for better closed loop performance using the roll stabilized frame. The actual simulations that will be used to produce the results presented later always use the body axis system of equations because the fins and aerodynamics are truly attached to the body.

VII. Alternate Autopilots

Four autopilots will be discussed. They are: a three loop in the body axis system; a three loop in the roll stabilized frame; a two loop in the body axis; and a two loop in the roll stabilized frame. Each will discussed in detail.

A. Three Loop in the Body Axis System

The equations for the fin commands for the three loop autopilot using body axis variables are:

$$\delta_Y = K_{IAy}\int (A_{y_m} - K_{ss}A_{y_c})\ \mathrm{d}t + K_\psi \int R_m\ \mathrm{d}t + K_r R_m$$

$$\delta_P = K_{IAz}\int (K_{ss}A_{z_c} - A_{z_m})\ \mathrm{d}t + K_\theta \int Q_m\ \mathrm{d}t + K_q Q_m$$

The subscript "m" is for measured. That is, these are measured quantities. This paper assumes a perfect Inertial Measurement Unit (IMU) in that the IMU is at the center of mass so there are no moment arm and there are no dynamics associated with the measurement device. It should be noted the output of the IMU is G's for acceleration. The block diagram of the pitch channel is presented in Figure 1.

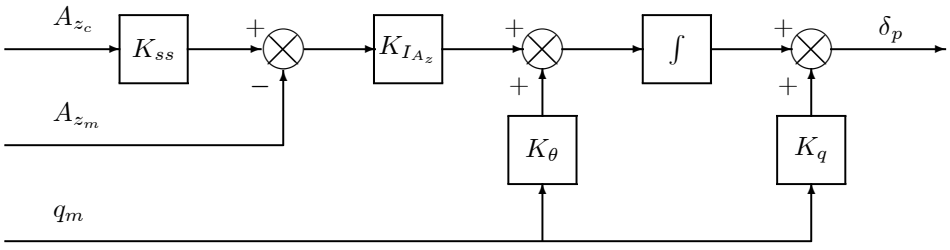

Figure 1. Three Loop Topology

B. Three Loop in the Roll Stabilized System

The equations for determining commands for this autopilot are first the deflections in the roll stabilized system are computed from

$$\hat{\delta}_Y = K_{IAy} \int \left(\hat{A}_{y_m} - K_{ss} \hat{A}_{y_c} \right) \, \mathrm{d}t + K_\psi \int r_m \, \mathrm{d}t + K_r r_m$$

$$\hat{\delta}_P = K_{IAz} \int \left(K_{ss} \hat{A}_{z_c} - \hat{A}_{z_m} \right) \, \mathrm{d}t + K_\theta \int q_m \, \mathrm{d}t + K_q q_m$$

Then these are transformed into the body fin deflections through

$$\delta_Y = \hat{\delta}_Y \cos(\phi) + \hat{\delta}_P \sin(\phi)$$

$$\delta_P = -\hat{\delta}_Y \sin(\phi) + \hat{\delta}_P \cos(\phi)$$

It should be noted the particular sign convention is used because the fin deflections are not a vector but in order to get the correct force or moment out of the fin the above signs must be used. The roll stabilized measurement variables are

$$\hat{A}_{y_m} = A_{y_m} \cos(\phi) + A_{z_m} \sin(\phi)$$

$$\hat{A}_{z_m} = -A_{y_m} \sin(\phi) + A_{z_m} \cos(\phi)$$

and

$$q_m = Q_m \cos(\phi) + R_m \sin(\phi)$$

$$r_m = -Q_m \sin(\phi) + R_m \cos(\phi)$$

The whole idea of this autopilot is to compute the fin deflections in the roll stabilized frame and modulate the output into the missile. The block diagram is the same as for the body axis.

C. Two Loop in the Body Axis System

The equations for the fin commands for the two loop autopilot are:

$$\delta_Y = K_{Ay} \left(A_{y_m} - K_{ss} A_{y_c} \right) \; + K_{rq} R_m$$

$$\delta_P = K_{Az} \left(K_{ss} A_{z_c} - A_{z_m} \right) \; + K_q Q_m$$

The block diagram of the pitch channel is presented in Figure 2.

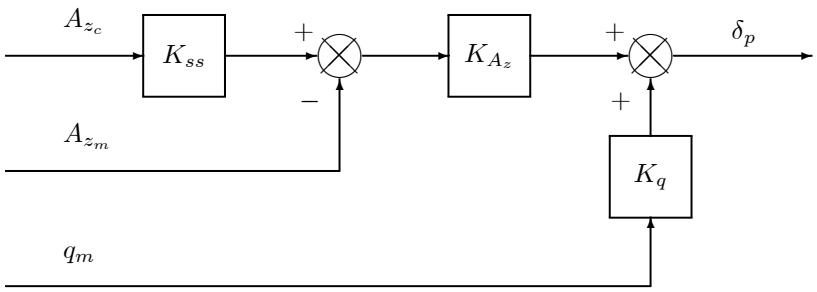

Figure 2. Two Loop Autopilot Topology

D. Two Loop in the Roll Stabilized System

The equations for the fin commands for the roll stabilized two loop autopilot are:

$$\hat{\delta}_Y = K_{Ay}\left(\hat{A}_{y_m} - K_{ss}\hat{A}_{y_c}\right) + K_r r_m$$

$$\hat{\delta}_P = K_{Az}\left(K_{ss}\hat{A}_{z_c} - \hat{A}_{z_m}\right) + K_q q_m$$

$$\delta_Y = \hat{\delta}_Y \cos(\phi) + \hat{\delta}_P \sin(\phi)$$

$$\delta_P = -\hat{\delta}_Y \sin(\phi) + \hat{\delta}_P \cos(\phi)$$

again

$$\hat{A}_{y_m} = A_{y_m}\cos(\phi) + A_{z_m}\sin(\phi)$$

$$\hat{A}_{z_m} = -A_{y_m}\sin(\phi) + A_{z_m}\cos(\phi)$$

and

$$q_m = Q_m \cos(\phi) + R_m \sin(\phi)$$

$$r_m = -Q_m \sin(\phi) + R_m \cos(\phi)$$

The block diagram is the same as for the body axis.

VIII. Simplified Example

The following simplifications were made in order to understand the basic dynamics of the closed loop systems. The effects of gravity are ignored, the x axis moment of inertia is zero ($I_{xx} = 0$). The forward velocity is constant, the pitch and heading angles are ignored and initially zero, the roll rate is constant. The y and z force was a linear function in sideslip or angle of attack respectively, The y and z moments are linear functions of both angle of attack or sideslip and pitch and yaw fin deflections. The dynamics were always computed in the body axis system. The dynamic equations are:

$$\alpha = \tan\left(\frac{W}{U}\right) \qquad \beta_M = \tan\left(\frac{V}{U}\right)$$

$$F_x = 0 \qquad F_y = Y_{\beta_M}\beta_M \qquad F_z = Z_\alpha \alpha$$

$$M_x = 0 \qquad M_y = M_\alpha \alpha + M_{\delta_P}\delta_P \qquad M_z = N_{\beta_M}\beta_M + N_{\delta_Y}\delta_Y$$

$$\dot{U} = 0 \qquad \dot{V} = \frac{F_y}{m} - RU + PW \qquad \dot{W} = \frac{F_z}{m} - PV + QU \tag{1}$$

$$\dot{P} = 0 \qquad \dot{Q} = \frac{M_y}{I} + PR \qquad \dot{R} = \frac{M_z}{I} - PQ \qquad \dot{\phi} = P \tag{2}$$

$$A_x = \frac{F_x}{mg} \qquad A_y = \frac{F_y}{mg} \qquad A_z = \frac{F_z}{mg}$$

Equations 1 and 2 are integrated in the nonlinear dynamics model to produce the states.

The aerodynamics are further simplified by

$$Y_{\beta_M} = Z_\alpha \qquad M_\alpha = -N_{\beta_M} \qquad M_{\delta_P} = N_{\delta_Y}$$

The specifics of the dynamics model are

Variable	Value	Description	Value
m	46.0	Mass	Kg
I	22	Moment of Inertia	Kg-m^2
Z_α	-4712.4	Force due to Angle of Attack	N
M_α	-549.8	Moment due to Angle of Attack	N-m
M_{δ_P}	-1570.8	Moment due to Fin Deflection	N-m
U	500	Forward Velocity	m/s
g	9.81	Gravity Constant used for Unit Conversion	m/s^2

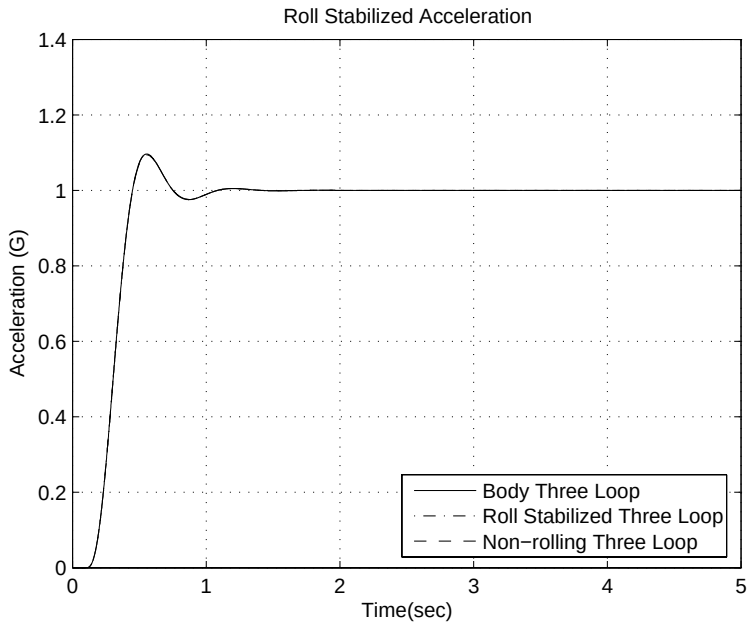

Figure 3. Roll Stabilized Acceleration

The autopilots were designed using a linear optimal control method. The specific gains for the three loop designs are

$$K_{IAy} = 1.3671 \qquad K_\theta = 2.4020 \qquad K_q = 0.2594 \qquad K_{SS} = 1.0345$$

and for the two loop designs are

$$K_{IAy} = 0.1650 \qquad K_q = 0.2197 \qquad K_{SS} = 1.2293$$

IX. Results

The first check was to make sure the autopilot design was implemented properly in the nonlinear simulation. An equivalent non-rolling linear planar simulation was run and the nonlinear simulations were run with the same aerodynamics and autopilot with the roll rate set to zero. The results were as expected. The nonlinear model reduces to the linear model when the roll rate is zero. The acceleration and fin deflections for the three loop system are presented in Figures 3 and 4. the two loop responses are presented in Figures 5 and 6

A. Roll Rate 0.2 Hz Commanded Acceleration 0.5 G's

The roll rate was set to 0.2 Hz and the acceleration command was set to 0.5 G's in the inertial z direction. The acceleration time histories are shown in Figure 7. This figure shows a slightly different view of the step response. The view is in an inertially fixed frame that is initially aligned with the body frame. The command is in the inertial z direction but the response can be out of plane. The desired response is to remain in the inertial x-z plane. As can be seen the three loop autopilot that is implemented in the body axis system is the only system that produces significant deviation from the desired response. At this low frequency the deviations might be deemed acceptable but both two loop and the roll stabilized three loop provides a better response.

The area at the end of the maneuver is expanded and is shown in Figure 8 and expanded even further in Figure 9. The three loop implemented in the body axis response also results in a steady state limit cycle of approximately the same magnitude as the three loop roll stabilized response. Notice that there is a small error in the two loop responses.

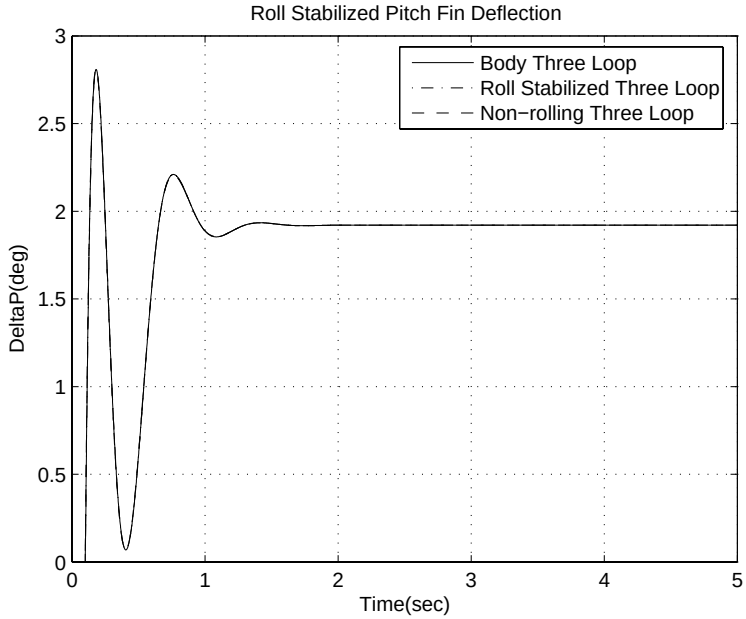

Figure 4. Roll Stabilized Pitch Fin Deflection

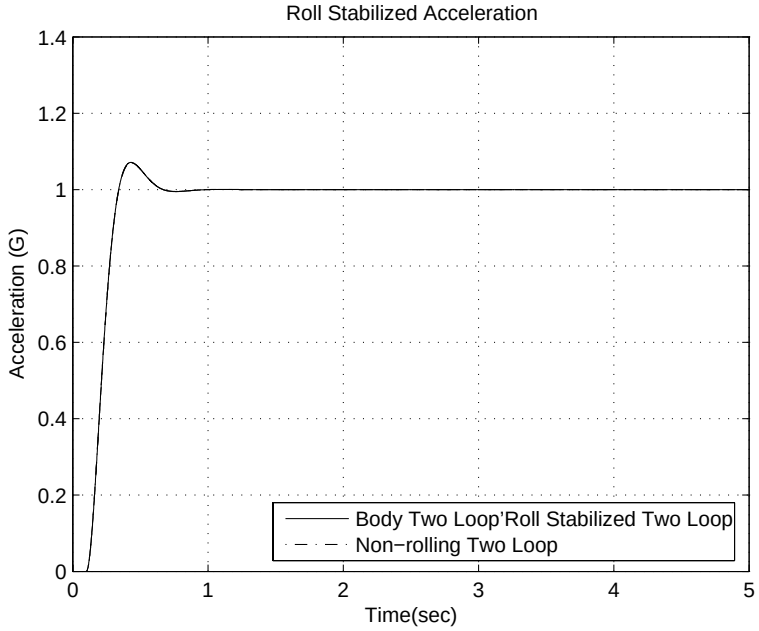

Figure 5. Roll Stabilized Acceleration

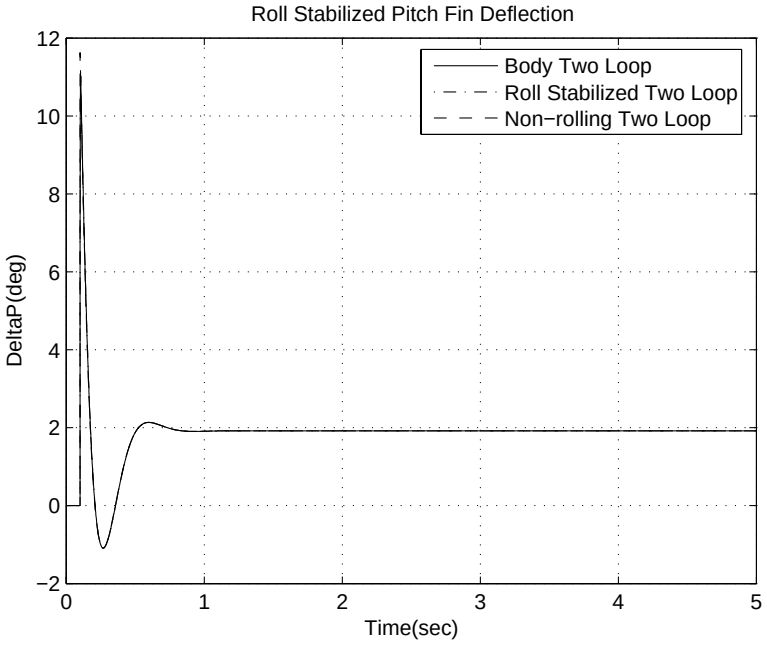

Figure 6. Roll Stabilized Pitch Fin Deflection

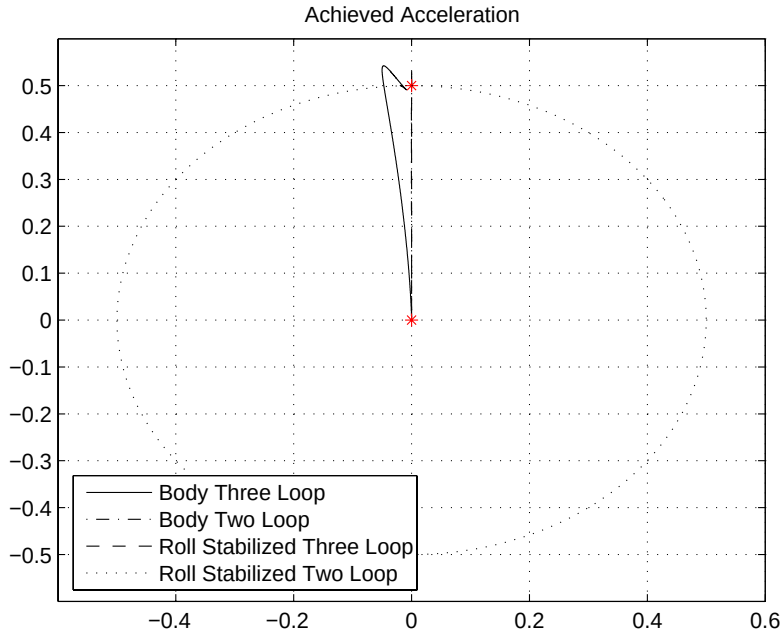

Figure 7. Achieved Acceleration

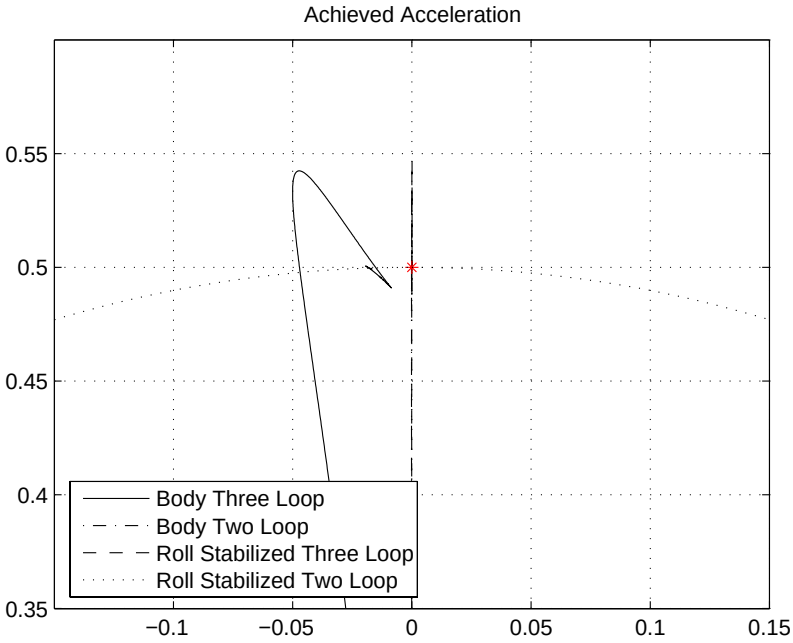

Figure 8. Expanded Achieved Acceleration

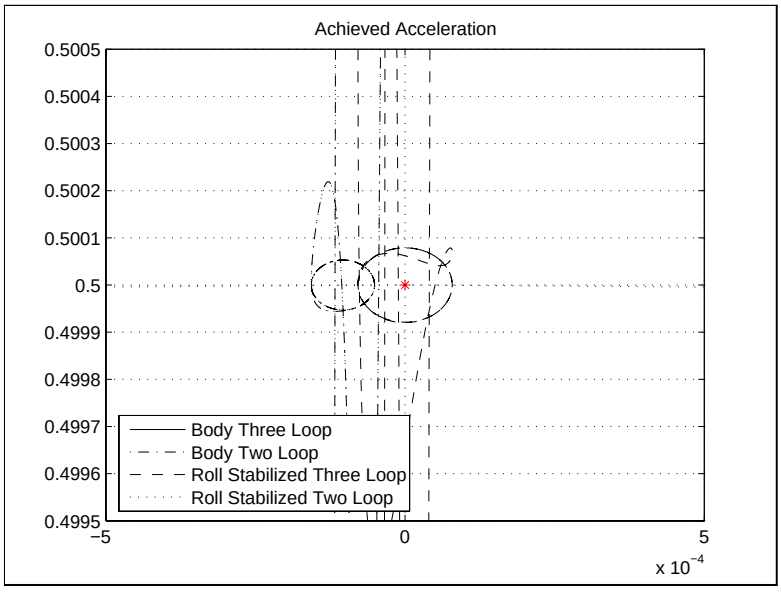

Figure 9. Further Expanded Acceleration

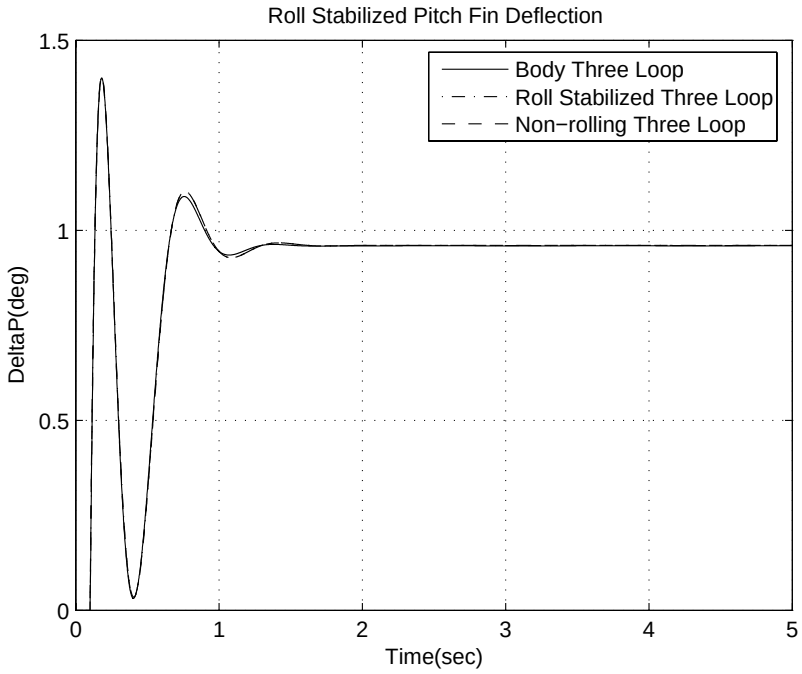

Figure 10. Roll Stabilized Pitch Fin Deflection

The roll stabilized fin deflections in the primary channel for both three loop autopilots are compared with the non rolling deflection that would produce the planar acceleration are shown in Figure 10.

The acceleration responses in the primary direction for the three loop autopilots is shown in Figure 11. The two loop designs are shown in Figures 12 and 13. The off axis fin deflections are presented in Figure 14.

B. Equivalence of Two Loop Closed Loop System

As can be seen by the results the two loop autopilot topologies are exactly the same because of the symmetry of this example. For the two loop autopilot based on the body axis, the fin deflections (removing the measurement notation) are

$$\delta_Y = K_{Ay}\left(A_y - K_{ss}A_{y_c}\right) + K_r R$$
$$\delta_P = K_{Az}\left(K_{ss}A_{z_c} - A_z\right) + K_q Q$$

and for the roll stabilized system

$$\hat{\delta}_Y = K_{Ay}\left(\hat{A}_y - K_{ss}\hat{A}_{y_c}\right) + K_r r$$

$$\hat{\delta}_P = K_{Az}\left(K_{ss}\hat{A}_{z_c} - \hat{A}_z\right) + K_q q$$

$$\delta_Y = \hat{\delta}_Y\cos(\phi) + \hat{\delta}_P\sin(\phi)$$
$$\delta_P = -\hat{\delta}_Y\sin(\phi) + \hat{\delta}_P\cos(\phi)$$

with

$$\hat{A}_y = A_y\cos(\phi) + A_z\sin(\phi)$$
$$\hat{A}_z = -A_y\sin(\phi) + A_z\cos(\phi)$$

and

$$q = Q\cos(\phi) + R\sin(\phi)$$

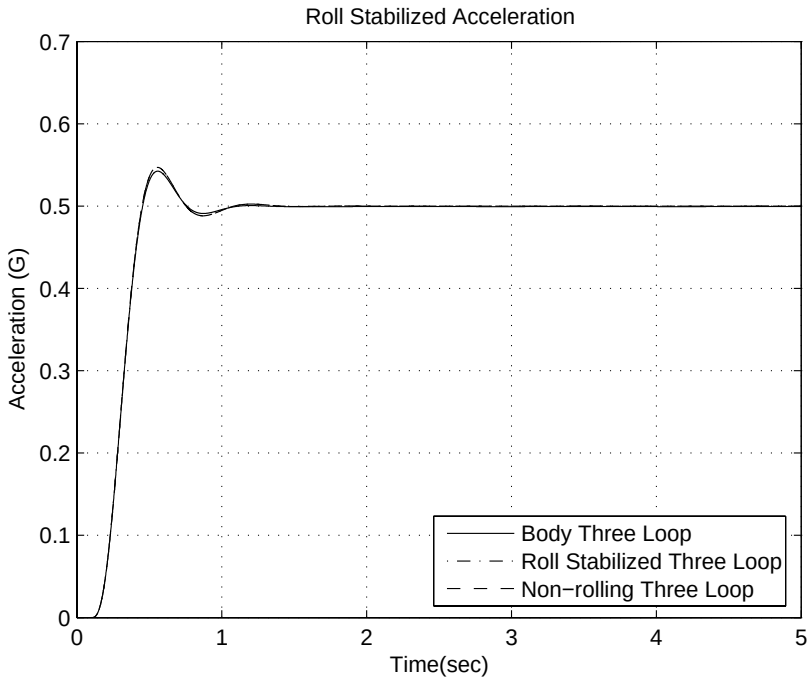

Figure 11. Roll Stabilized Acceleration

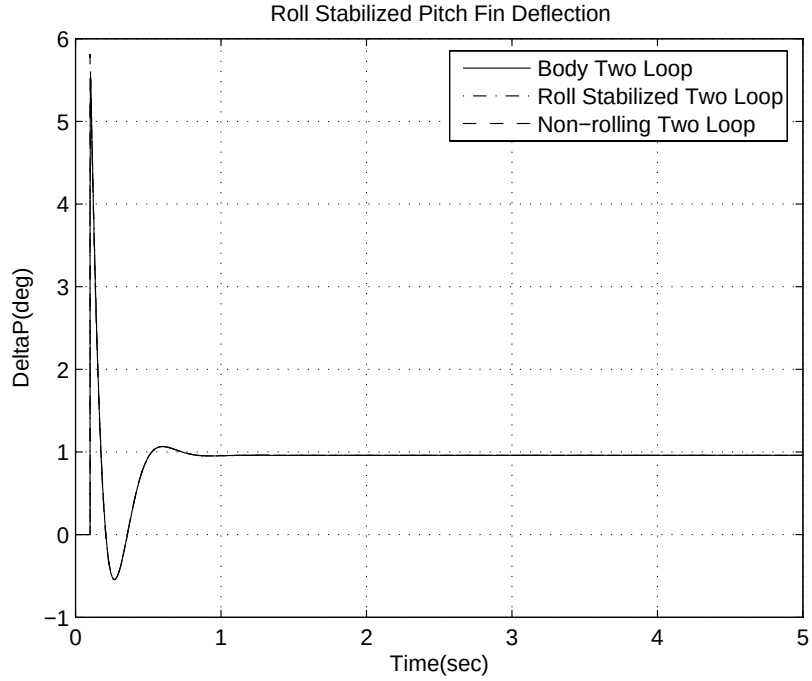

Figure 12. Roll Stabilized Fin Deflection

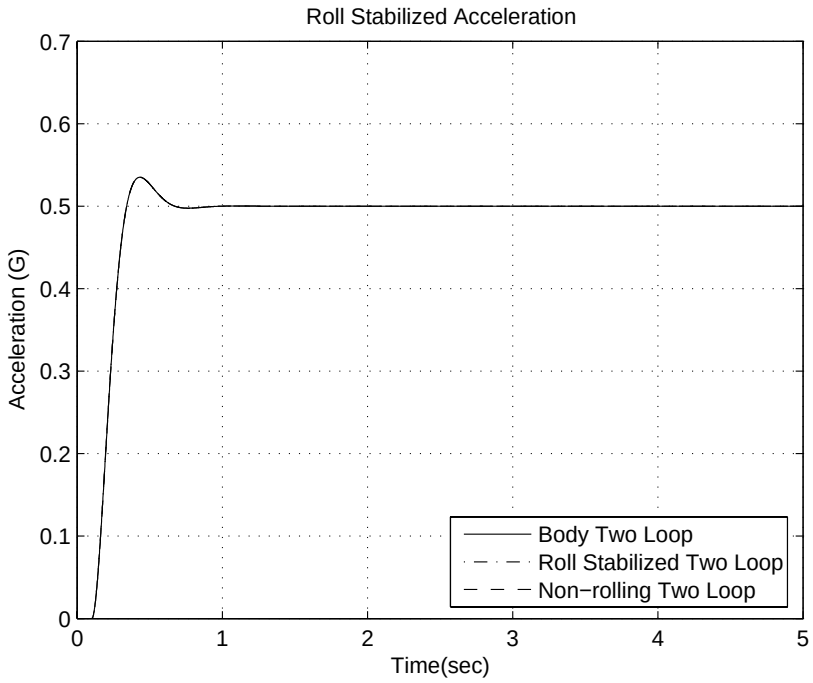

Figure 13. Roll Stabilized Acceleration

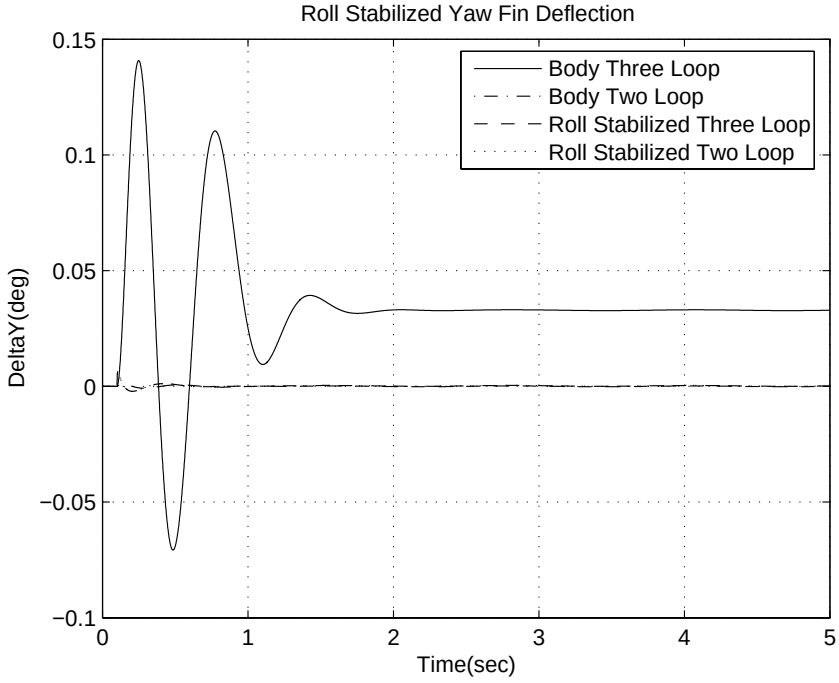

Figure 14. Roll Stabilized Yaw Fin Delflection

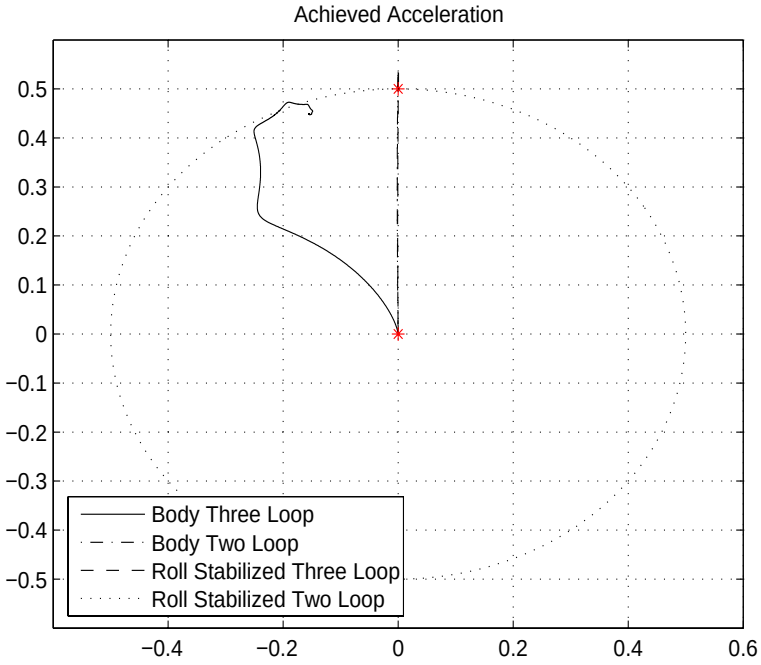

Figure 15. Achieved Acceleration

$$r = -Q\sin(\phi) + R\cos(\phi)$$

Going through the algebra it can be shown the two loop designs are exactly the same. The three loop designs are not because of the integrator in the loop.

C. Roll Rate 2.0 Hz Commanded Acceleration 0.5 G's

The roll rate was set to 2.0 Hz and the acceleration command was set to 0.5 G's in the inertial z direction. The acceleration time histories are shown in Figure 15. As can be seen the three loop autopilot implemented in the body axis system is significantly worse than the other three autopilots.

The area at the end of the maneuver is expanded and is shown in Figure 16. Notice how the axis are of a different scale then the previous plot. The limit cycle magnitude has increased for all the autopilots, including the body based three loop autopilot which is not shown.The same set of results as previously presented are shown in Figures 17 to 21.

D. Roll Rate 2.0 Hz Commanded Acceleration 5.0 G's

It was desired to see the effect of increasing the commanded G's. The roll rate was set to 2.0 Hz and the acceleration command was set to 5.0 G's in the inertial z direction. The acceleration time histories are shown in Figure 22. As can be seen the overall response is slightly different.

The area at the end of the maneuver is expanded and is shown in Figure 23

E. Roll Rate 2.0 Hz Non-Zero X Moment of Inertia

It was desired to investigate the effects of having non zero x moment of inertia. The nonlinear equations were used instead of the simplified equations. The results are presented in Figures 24 through 26.

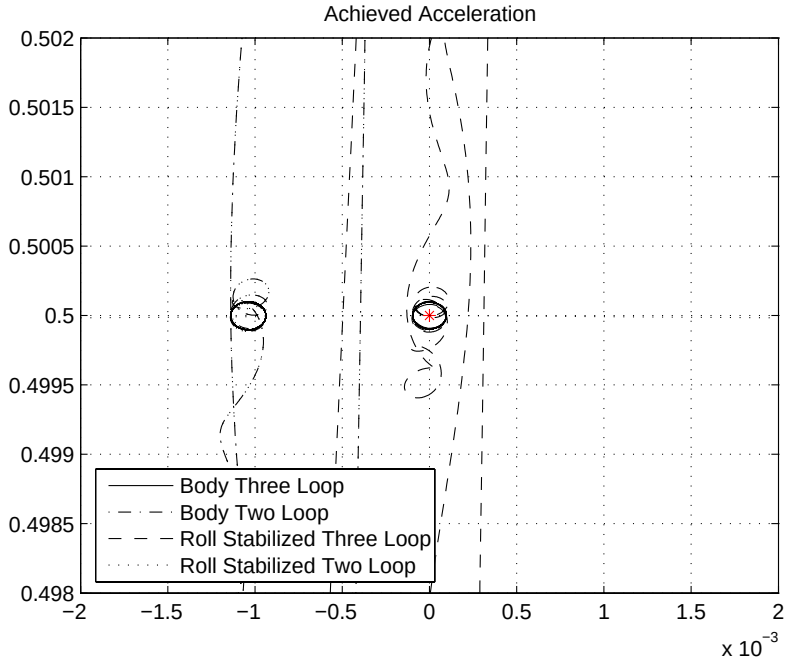

Figure 16. Acieved Acceleration

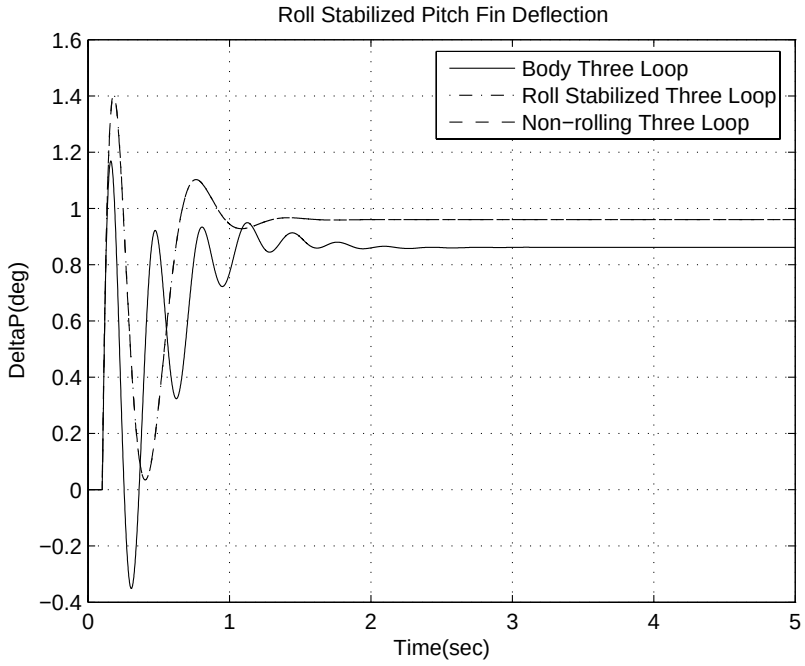

Figure 17. Roll Stabilized Pitch Fin Deflection

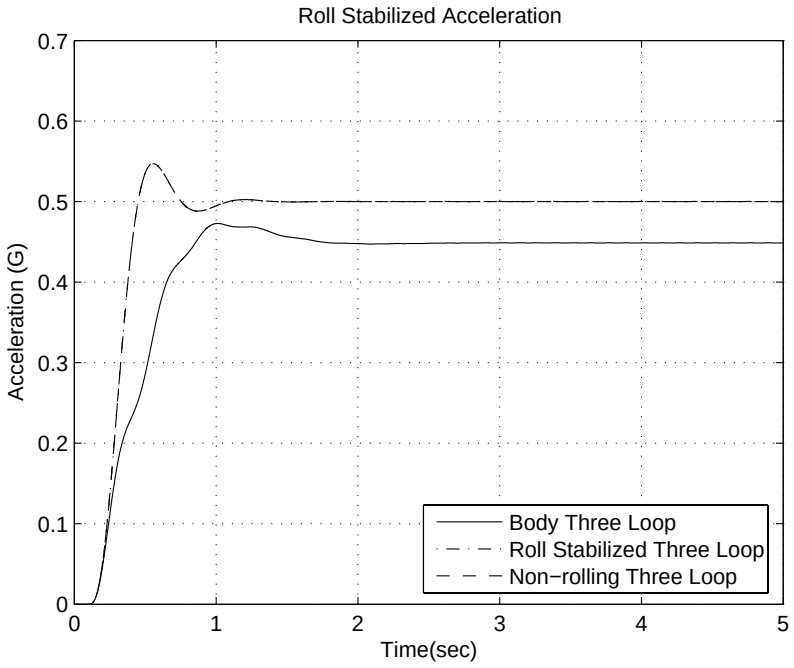

Figure 18. Roll Stabilized Acceleration

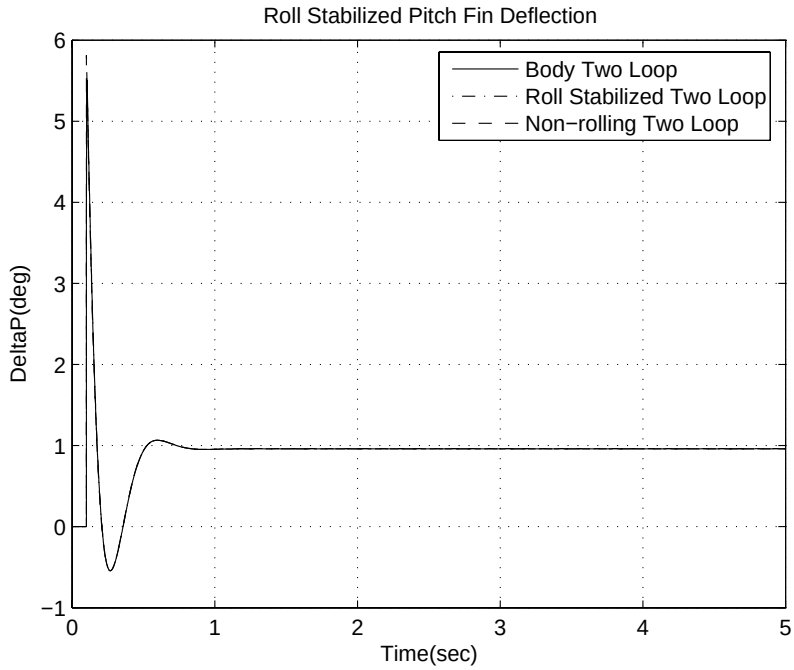

Figure 19. Roll Stabilized Pitch Fin Deflection

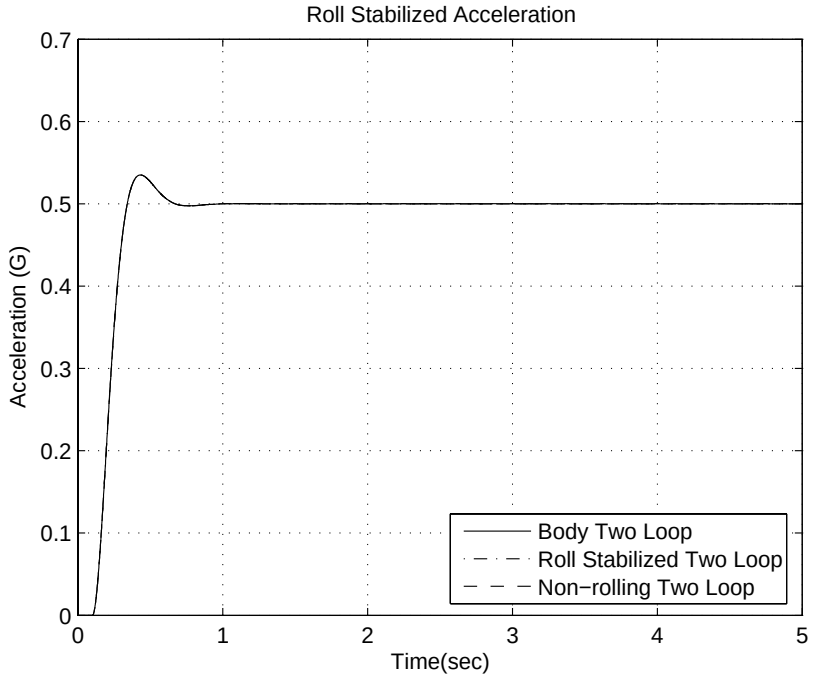

Figure 20. Roll Stabilized Acceleration

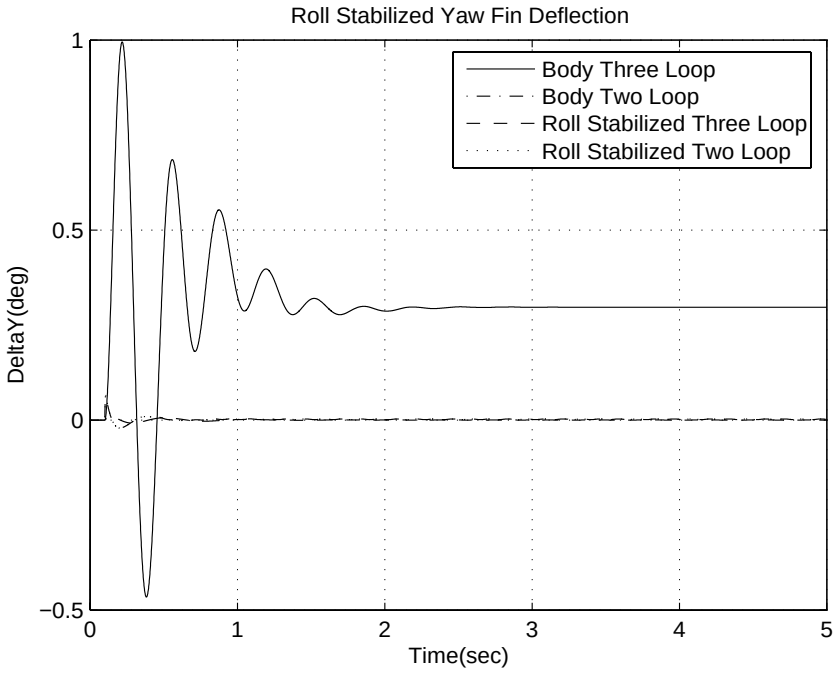

Figure 21. Roll Stabilized Yaw Fin Deflection

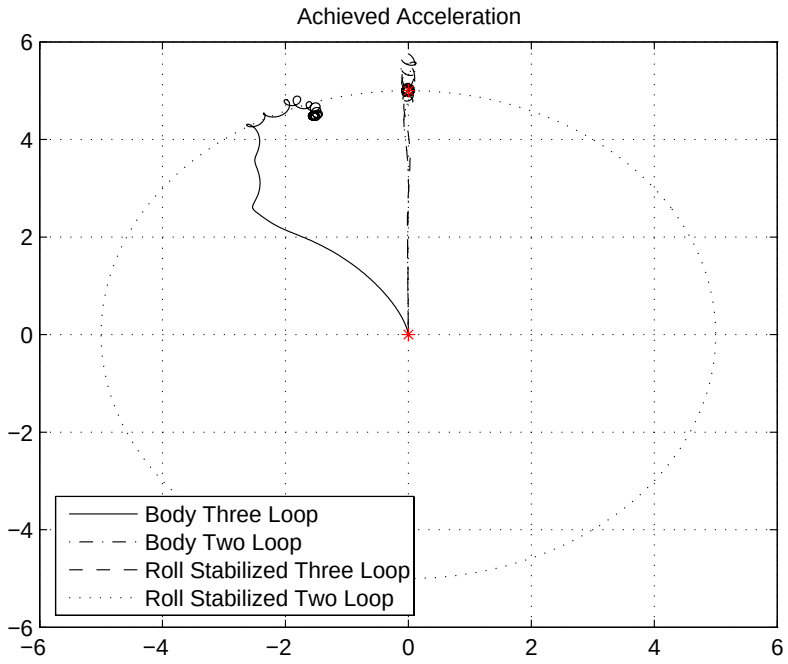

Figure 22. Achieved Acceleration

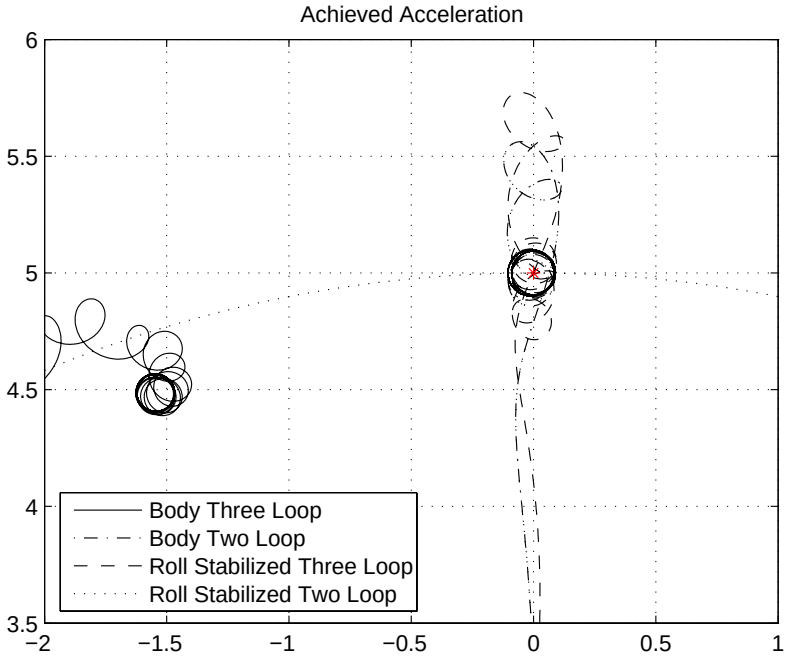

Figure 23. Expanded Achieved Acceleration

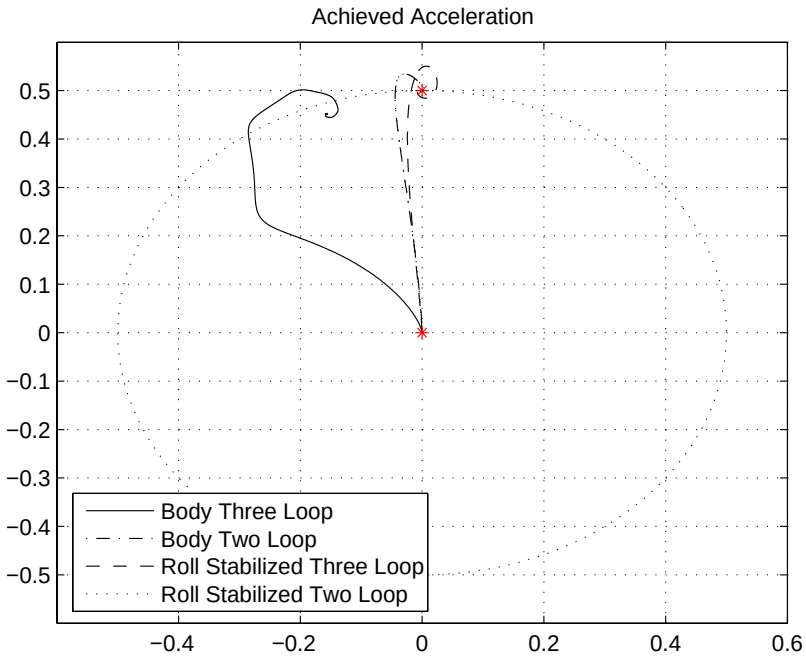

Figure 24. Achieved Acceleration

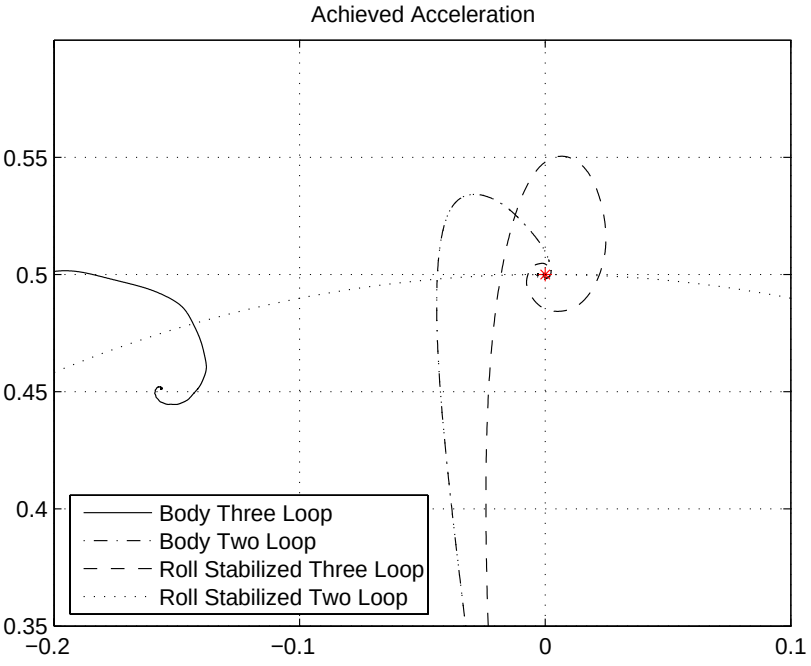

Figure 25. Expanded Achieved Acceleration

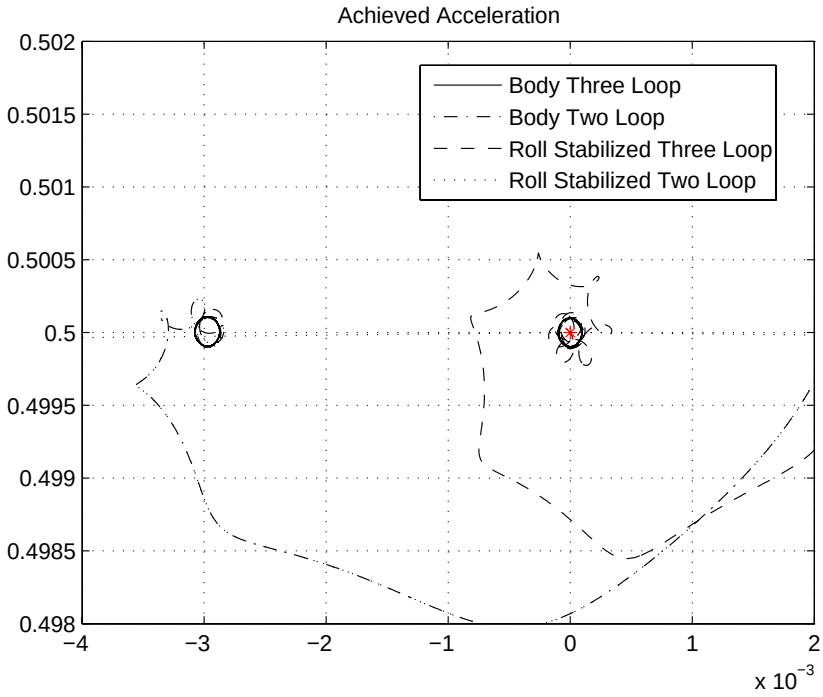

Figure 26. Further Expanded Achieved Acceleration

F. Very High Roll Rates

The effect of increasing the roll rate significantly beyond the bandwidth of the closed loop system will now be investigated. Fist we must determine the closed loop transfer functions of the non-rolling airframe and controller. The closed loop transfer functions can be determined from the open loop system and the feedback gains. The two loop acceleration achieved to acceleration command is given by

$$\begin{aligned}\frac{A}{A_c} &= \frac{151.2013}{s^2 + 15.8891s + 151.2013} \\ &= \frac{151.2013}{(s + 7.9446 + 9.3854i)\,(s + 7.9446 - 9.3854i)}\end{aligned}$$

Since this is a second order speed of response is determined by the distance of the complex poles from the origin. The closed loop system bandwidth is approximately 2.0 Hz. The three loop systems closed loop transfer function

$$\begin{aligned}\frac{A}{A_c} &= \frac{1054.5}{s^3 + 18.7s^2 + 200.3s + 1054.5} \\ &= \frac{1054.5}{(s + 4.6814 + 9.5242i)\,(s + 4.6814 + 9.5242i)\,(s + 9.3623)}\end{aligned}$$

The bandwidth of this system is approximately 1.8 Hz. The roll frequency is increased to 10 Hz. The results are somewhat surprising in that both three loop topologies degrade significantly. The two loop has degraded but not nearly as much as the three loop. The x moment of inertia is again neglected and the commanded accelerations returned to 0.5 G's. The acceleration results are presented in Figure 27. The x moment of inertia is again set to 5 and the results are show in Figures 28. These show the three loop body based autopilot is not performing, the higher roll rate just makes the response further from the desired. The roll stabilized three loop autopilot is degrading to an almost neutrally stable solution by 10 Hz and has crossed over to unstable by 20Hz. The two loop autopilot has significantly better performance at these higher roll

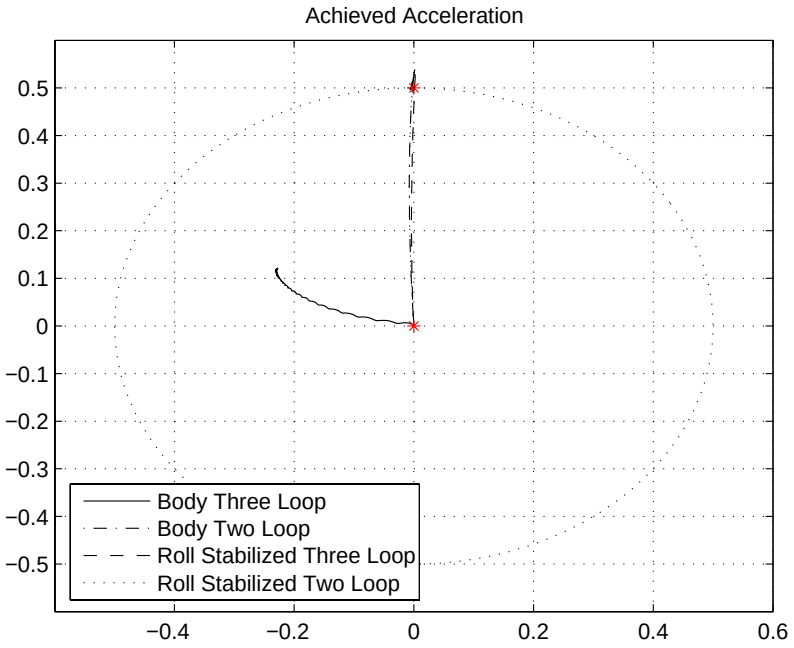

Figure 27. Achieved Acceleration

rates with the x moment of inertia present, even though it does not produce a limit cycle around the desired set point.

X. Conclusion

Four autopilot topologies were examined for control of a rolling airframe. These were the classical three loop implemented in the body axis system, the classical three loop implemented in a roll stabilized system and a two loop autopilot implemented in both the body and roll stabilized frames. It is shown the two loop implementations are identical. There is no advantage of using the roll stabilized coordinate frame for the two loop design. The three loop autopilots produce significantly different results. For this example, all autopilot formulations provided adequate responses for a slowly rolling airframe. The example had the body roll rate at one tenth the bandwidth of the closed loop system. The body based autopilot, even at this low roll rate, showed deviation from the desired response. The deviation of this implementation continued as the roll frequency increased . Under no conditions did the system become unstable. The roll stabilized three loop system performs well while the roll frequency remains below the closed loop bandwidth of the airframe. At ultra-high (ten times the closed loop bandwidth) roll rates the system went unstable. The two loop autopilot performed better at the ultra high frequencies. This system did not show signs of instability until the airframe roll rate was greater than 50 Hz. Zero steady state error was not achieved for the two loop autopilot but it remained small under all conditions except when the airframes roll rate was larger than 50 Hz. It should be noted a first order 160 Hz control actuation system was included in all models in order to remove the algebraic loop in the simulation.

References

[1]Roskam, Jan Airplane Flight Dynamics and Automatic Flight Controls Part I, Darcorp, Inc., 1995. pp 13-14

[2]Etkin, Bernard,Dynamics of Flight, Second Ed.,John Wiley and Sons Inc. 1982 Page 93

[3]Blakelock, John H. Automatic Control of Aircraft and Missiles Second Edition, John Wiley and Sons Inc. 1991, pp 8-17

[4]Duane McRuer, Irving Ashkenas, and Dunstan Graham, Aircraft Dynamics and Automatic Control, Princeton University Press, 1973

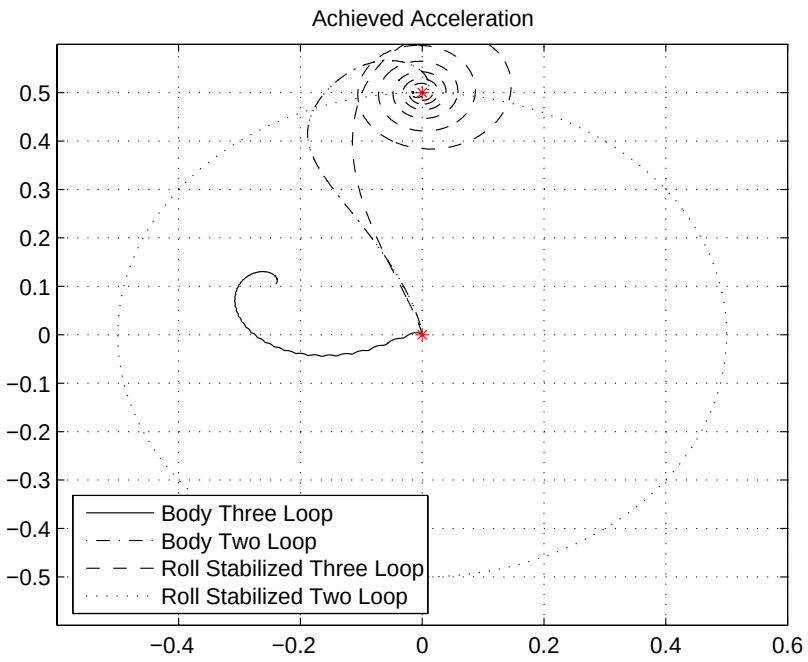

Figure 28. Achieved Acceleration

[5]Malyevac, D.S. and W.R. Chadwick ERGM LBFT1 Guided Flight Phase Post Flight Analysis,. Naval Surface Warfare Center, Dahlgren Division, Dahlgren, Virginia, Nov 2003